Journal of Medical Robotics Research, Vol. 0, No. 0 (2024) 1–?? © World Scientific Publishing Company

Training with a Visual-Haptic Simulator for Trocar Insertion

Andres Hassun¹, Kimberly Kho², M. Yvette Williams-Brown³, and Ann Majewicz Fey^{1,2,3} *

Trocar insertion is a critical first step of all minimally invasive surgery; however, it also carries a high risk for errors. Studies suggest that entry errors are the most common complication in laparoscopic surgery with 4% of errors leading to patient fatality. Surgeon error due to excessive force is often the cause for entry errors; however, adequate training has been shown to reduce the risk of these surgical errors. In practice, institutions lack widespread and relatively inexpensive means to train surgeons for trocar entry that does not involve patient risk. In our prior work, we presented a simple Stewart platform haptic device with a numerical model to simulate key force characteristics of trocar insertion. Evaluation in our first study was limited to device characterization. In this paper, we present a more robust haptic mechanism with higher fidelity linear actuators, an increased workspace, and tissue visualization to accompany haptic cues. We also present a novel upper module that allows for a sudden drop of the trocar after the final puncture event to create a more realistic simulation. We performed a user study with eight novices to investigate how well the device and visualization train users in the trocar insertion procedure. By the end of the experiment, subjects using the device had a normalized error reduction of roughly 85% on average, relative to themselves. This device shows potential for widespread training of trocar insertion, possibly leading to fewer complications and deaths following the procedure. Finally, our upper module also represents an innovative addition for traditional admittance-type haptic device designs, not typically capable of accurately representing motion in free space.

Keywords: Trocar Insertion; Surgical Training; Kinesthetic Haptic Simulator; Laparoscopic Surgery

Changes may be found in the abstract, and sections 2.1, 2.2, 2.3, 2.4, 4.2, 5, 6, and 7. All changes are marked in red.

1. INTRODUCTION

The initial steps of laparoscopic surgery involves inserting a trocar, a sealed, hollow cylinder with a tapered tip, into the abdomen. Once inserted, carbon dioxide is pumped into the abdomen to improve ease of access and visibility inside the body for the surgeon. Other medical devices and tools can then enter the body through the trocar and be used in the surgical procedure. Benefits of laparoscopic surgery include faster recovery times and decreased blood loss. However, most injuries in laparoscopic surgeries occur during the trocar insertion, with some studies indicating laparoscopic entry injuries as high as 3.3 per 1,000.² Additionally, the reported overall complication rate varies between 0.2% and 10.3%, with the diagnosis of a majority of these injuries coming days after the initial surgery.³ Roughly 4% of these injuries result in patient fatality.⁴ As for hospital liability, a study in the Netherlands found that about 20% of laparoscopy related claims are due to entry-related complications.⁴ Many of these injuries occur due to the lack of visual feedback available to the surgeon during insertion. Instead,

the surgeon must depend on their sense of touch and kinesthetic feedback from the trocar to avoid causing intestinal, urological, or vascular injuries. To exacerbate the issue, patients have high variability in the force and displacement needed to gain abdominal entry. For example, elderly patients may have less elastic tissue, and obese patients have a greater distance required for travel to enter the abdomen, as well as a thicker peritoneum, the final tissue layer to enter the surgical cavity.⁵

In clinical practice, trocars with clear plastic tips have gained popularity to help visualize the tissue layers by inserting the endoscopic camera into the trocar prior to insertion. These trocars have been shown to decrease the odds of injury, ⁶ though most evaluation studies only consider obese patients. ^{7,8} Additionally, due to the primarily kinesthetic nature of trocar insertion, the increase in visual assistance does not necessarily eliminate the need for force-based training. Medical simulators are promising as they allow surgeons and students to train for a given procedure without risking harm to a real patient. ⁹ In addition, parameters of these computer-based simulators can be adjusted to better represent the diverse patient population.

^{*}This work was supported in part by NSF #2109635 as an REU supplement to support A. Hassun. ¹ A. Hassun and A. Majewicz Fey are with the Department of Mechanical Engineering at the University of Texas at Austin, TX 78712 USA (email: Ann.MajewiczFey@utexas.edu). ² K. Kho and A. Majewicz Fey are with UT Southwestern Medical Center, Dallas, TX 75390, USA. ³ M. Y. Williams-Brown and A. Majewicz Fey are with Dell Medical School, Austin, TX 78712, USA.

Previous attempts to develop simulators for trocar insertion include the development of complex tissue models using neural networks and finite element methods. ¹⁰ Although accurate, these methods are computationally expensive, and therefore difficult to implement in a standalone device that could be widely distributed. Medical simulators with force feedback, such as the TroSim, have been shown to improve the success rate of trocar insertion when evaluating subjects with no previous trocar experience. ¹¹ Although the TroSim provides a 3D scene with a human body and trocar, it does not provide visualization of the different layers of tissue modeled which is a critical aspect of training.

This paper builds on previous work performed by our group to present a low-cost haptic simulator for trocar insertion using a Stewart platform.¹² We expand our prior work by integrating higher fidelity linear actuators, creating visualization of the tissue layers to accompany the device, and performing a human subject study to verify the effectiveness of the simulator in training trocar insertion skills. In addition, we created a novel dropping mechanism, called the upper module in this paper, which enables a free falling sensation once the simulated peritoneum has been punctured. This overcomes an inherent limitation of admittance-type haptic devices to accurately render free space. We show that our device is capable of mimicking trocar insertion forces in a package that is more affordable and portable than other training simulators. Through our findings, we hope to more effectively train surgeons and decrease the number of complications occurring in laparoscopic surgeries.

2. HAPTIC DEVICE DESIGN

The trocar simulator is an admittance-type haptic device based on a Stewart platform, a six degree of freedom parallel manipulator. Recently, Stewart platforms and other parallel mechanisms have garnered interest in the area of robotics and manufacturing, ¹⁴. ¹⁵ Due to the admittance structure of the simulator, the device renders the large forces of a virtual wall more closely than more common impedance haptic devices by recording force as the input and outputting a corresponding displacement. ¹³ The high forces needed during trocar insertion makes a Stewart platform a good choice for this application.

2.1. Mechanical Assembly

The trocar simulator, shown in Fig. 1, is actuated with six Firgelli Automation Feedback Rod Linear Actuators. The device is more than capable of simulating the forces found in a typical trocar insertion with a dynamic force of 156 N for each motor, totalling 936 N. The linear actuators mount to the base of the device and are able to rotate slightly as the platform moves. Additionally, the linear actuators attach to the primary platform using ball joints. The flexibility of the attachment points allows slight movement of the linear actuators to prevent the Stewart platform from binding. Due to the admittance type structure of the device, a 1 degree of freedom, TAL220 Parallel Beam 10 kg Load Cell mounts onto the primary platform, which interfaces

with a RobotShop Wheatstone Amplifier Shield, to input the external, user-applied, force. The linear actuators then output the calculated displacement. A 3D printed model of a 12 mm diameter trocar mounts into a holder above the load cell and is allowed to freely rotate. To train with different geometries of trocars, the 3D model trocar may be easily switched out for an alternate model. While this study is limited to a single degree of freedom, the Stewart platform design allows us to more realistically and accurately simulate the procedure by rendering both the 3 DOF forces and 3 DOF torques important in trocar insertion without significantly altering the design of the device.

Another important aspect of trocar insertion is to quickly stop insertion as soon as the trocar "pops" through the peritoneum. Unfortunately, admittance type haptic devices are notorious for their the inability to render free space accurately. Thus, we developed a novel mechanism on top of the primary platform, referred to as the upper module. The load cell and model trocar are attached to three vertical rails. For each rail, an extended solenoid locks the load cell and model trocar at the rail's highest point. Once the user punctures the simulated peritoneum region, the solenoids retract, causing the load cell and model trocar to fall 18 mm along the rails before contacting a damping foam, thus creating a simulated region of free space.

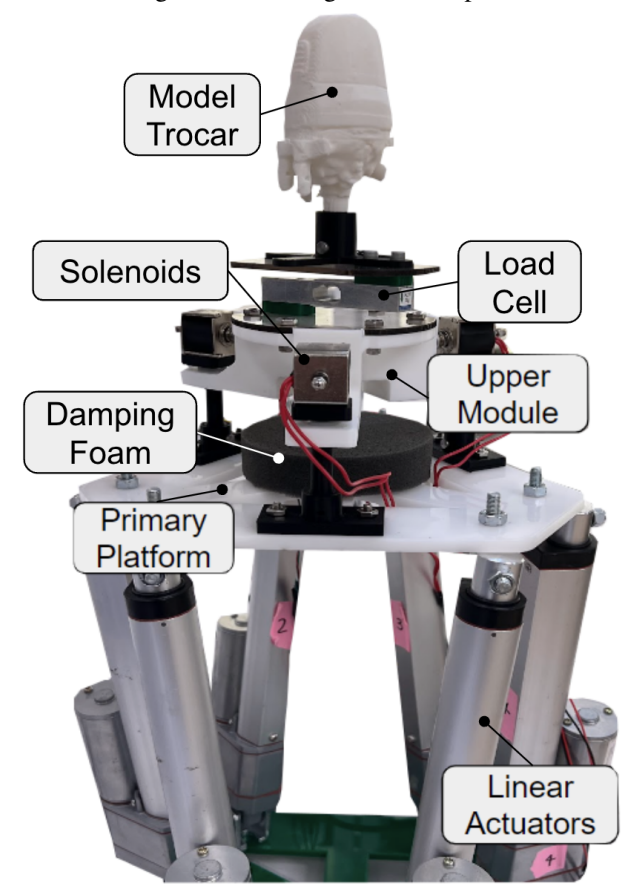


Fig. 1: Full assembly of the trocar simulator.

2.2. Control of Device

An Arduino Due micro-controller controls the linear actuators, reads the force input from the load cell, and reads the position feedback from each linear actuator's potentiometer. All inputs are read using a moving average filter with a window size of 10 samples to reduce susceptibility to noise. The controller uses an energy based model, taking the force input, F, and displacement, x, during each control loop's iteration, n, to determine the correct phase of tissue. Eq. 1 shows the calculation of the user's energy, W, into the system. The simulator enters the next phase upon reaching certain energy thresholds, changing spring, k, and damping parameters, b, shown in Eq. 2, and calculating the displacement and velocity accordingly.

Because Stewart platforms tend to have instability at low inertias, the controller uses a proportional, integral, and derivative (PID) loop^{16, 17} to improve feedback loop stability. Although the Stewart platform can move with six degrees of freedom, the current load cell limits the device to a vertical, linear displacement and thus simplifies the controls calculations.¹⁸

$$W_n = W_{n-1} + F_n(x_n - x_{n-1}) \tag{1}$$

$$\begin{cases} k_1 = (0.09x + 0.1)/1.25 & b_1 = 0.1, \text{ Phase I} \\ k_2 = (0.06x + 0.456)/1.1 & b_2 = 0.3, \text{ Phase II} \\ k_3 = 2 & b_3 = 0.3, \text{ Phase III} \end{cases} \tag{2}$$

2.3. Description of the Training Procedure

The training begins with light contact of the simulated abdomen and ends with puncturing into the abdomen. To engage with the simulator, the user lightly grasps the model trocar and gradually apply and increase their downward force to displace the simulator, as if performing a real trocar insertion. As they apply force, the user feels the stiffness change as they puncture through the different layers of tissue. The user continues until puncturing through the peritoneum layer, signified by the upper module dropping and a sudden decrease in the amount of force required for additional displacement of the linear actuators. The procedure is shown concisely in Fig. 2. Force, displacement, velocity, and time data of each trial is recorded, and a visualization can be provided to give the user visual feedback.

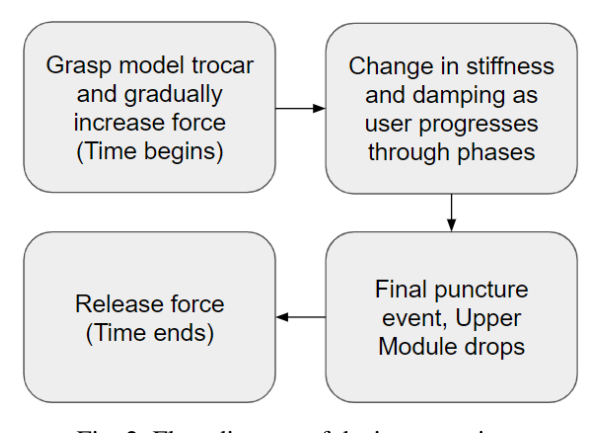


Fig. 2: Flow diagram of device operation.

2.4. Description of Visualization

The visualization, shown in Fig. 3, uses a deformable gel based model developed using the Chai3D haptic library to represent the human abdomen. 19 A sphere, which represents the tip of the trocar, interacts with the gel layers and punctures through the different layers as the device advances through the corresponding tissue phases. The Arduino sends the displacement information from the device in order to determine the position of the tool tip as it moves through the layers of tissue. The model is seen from an elevated side view, while a picture-in-picture display shows a close-up of the current layer as seen from the trocar tip. This viewpoint is particularly important as it simulates the endoscopic camera view available with clear-tipped trocars. The user can swap the main and picture-in-picture display at any time, but the trocar tip display should become the user's primary viewpoint as they progress through their training because of its closer similarity to the endoscopic camera view in real world situations. Users should be able to draw parallels between the force they apply to the simulator and the visual feedback provided to them by the movement through the gel layers.

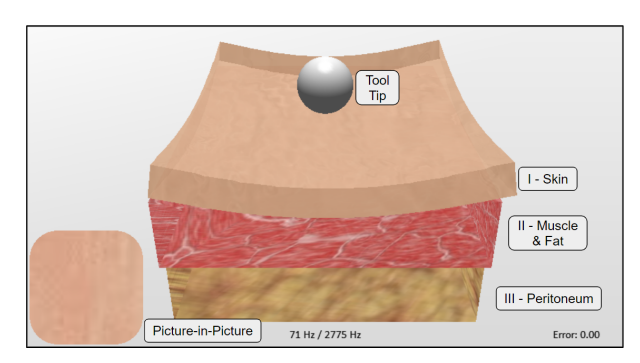


Fig. 3: Chai3D visualization of abdominal wall structure.

3. Insertion Model

To accurately simulate the trocar insertion procedure, we continue the work performed by Aldo *et al.*¹² and separately model the three phases of tissue by following a characteristic insertion curve, Fig. 4, and by applying stiffness and damping parameters specific to each phase.

3.1. Phases of Tissue

Three distinct phases of tissue, skin, muscle and fat, and peritoneum, shown in Fig. 3, emerge when analyzing the force profile of trocar insertions, each separated by a puncture event. A puncture event occurs after cutting through a layer of tissue and results in a short region of relatively lowered stiffness at the beginning of the next layer.

The first of the three phases, skin, is where most abdominal deformation occurs, and lasts until the first puncture event. The next phase, muscle and fat, can be treated as a homogeneous layer due to the continuous force profile. Additionally, maximum stiffness for the entire procedure occurs just before the

puncture event at the end of this phase. The final phase, the peritoneum, is the thinnest phase and has a relatively lower stiffness compared to the previous phase. However, puncturing too far past this phase or with too high of a velocity can cause damage to the organs underneath. Because each tissue phase has unique deformation properties, we separate the different phases in the numerical model outlined in the following section.

3.2. Numerical Model

As with the previous iteration, we use the characteristic force profile, Fig. 4, of a trocar insertion²⁰ and fit a piece-wise polynomial, Eq. 3, to represent the different phases and map force applied to the trocar, F_{app} , to the displacement from the top of the skin, x. Because puncture events do not occur at set displacement values, we use an energy-based model, which calculates the area under the force-displacement curve as the elastic energy directed into the system. Then, after reaching previously defined energy thresholds, the device simulates a puncture event and proceeds to the next phase.¹² Although the trocar simulator could use a higher fidelity model, this method has low computational costs, and thus allows for a quick haptic loop, and consequently, a smoother simulation.

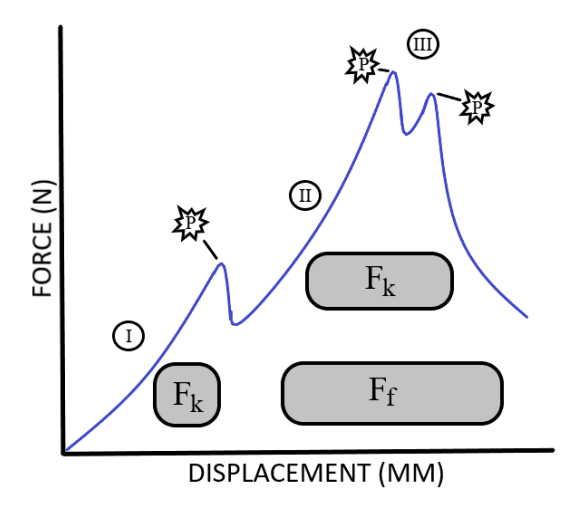


Fig. 4: Characteristic insertion curve of insertion. F_k and F_f represent the presence of stiffness and frictional forces respectively, and P denotes the puncture events. ¹²

$$F = \begin{cases} F_{app} - k_1 x - b_1 \dot{x}, & \text{if Phase I} \\ F_{app} - k_2 x - b_2 \dot{x}, & \text{if Phase II} \\ F_{app} - k_3 x - b_3 \dot{x}, & \text{if Phase III} \end{cases}$$
(3)

3.3. Haptic Rendering

Our new device makes the same assumptions as the previous iteration, ¹² where the training simulation begins and ends with continuous contact with the device and the configurations of the

virtual tool and haptic device are equivalent. To find our stiffness parameters, we differentiate the characteristic curve with respect to x, resulting in the K(x) shown in Eq. 2. We include constant damping parameters to improve the stability and realism of the device, with phase I containing a lower damping value than the other two phases because the trocar is assumed to be external to the tissue during this portion of the process. We use the parameters in conjunction with the force input from the load cell to find the corresponding velocity and displacement by applying the forward Euler method.

With this information, the device employs the control loop found in Algorithm 3.3.

Require: Inputs F_{app}, x_n, x_{pot} $B, K \leftarrow x_n$ $\dot{x} \leftarrow B, K, F_{app}, dt$ $x_{n+1} \leftarrow \dot{x}, x_n, dt$ $W_{app} \leftarrow F_{app}, x_{n+1}, x_n$ if $W > E_{Break}$ then Next Phase end if if Phase > 3 then Retract Solenoids end if $x_{PID} \leftarrow x_{n+1}, x_n, x_{pot}, dt$ return x_{PID}, \dot{x}

4. EXPERIMENTAL METHODS

To evaluate the effectiveness of the trocar simulator as a training tool, we performed novice human subject experiments both with and without the visualization in a study approved by the UT Austin IRB (#STUDY000000278). We expect the visualization to help decrease the elapsed time and displacement error of novices more quickly than those who train without the visualization, but for both conditions to improve novice performance across several trials.

4.1. Participants

For our participants, we chose eight novices who have no prior experience performing a trocar insertion. Participants performed a pre-experiment survey so we could gather information on their age, gender, handedness, and experience with interactive devices. Additionally, participants were given a post-experiment survey to evaluate their experience with the device.

Of the eight participants, all subjects were between the ages of 20 and 30. Seven participants were predominantly right-handed, with the final participant being left-handed. Finally, seven of the subjects are male.

4.2. Experimental Protocol

Prior to the experiment, participants were given instructions to gradually increase their applied force and stop when they feel as though they punctured through the peritoneum. They were then shown a brief demonstration of the device in operation, but they

did not perform training trials. Each subject was tasked with determining the required amount of force for themselves. The top of trocar simulator rested lower than shoulder height of the subject, and shorter subjects were provided a stepping stool. Each participant completed ten trocar insertion trials with the device. A set of five trials used the visualization, and five trials did not provide access to the visualization. The order of the conditions was randomized for each subject, and the subjects took a short break between the sets. The participants wore noise-cancelling headphones to prevent any sound from the trocar simulator from becoming distracting, and the majority of the trocar simulator was hidden from each subject's view in order to prevent additional audio and visual feedback from affecting a subject's interaction with the device.

4.3. Data Collection and Analysis

Before each subject began their experiment, the trocar simulator calibrates itself to compensate for possible inconsistencies with the maximum and minimum values in each linear actuator's potentiometer and provide the most accurate data possible. From each trial, we recorded the force, displacement, velocity, and time data within the same program as the visualization. When a trial ends, the data was saved into a CSV file. From this data, we can plot the average force vs. displacement curve of all trials and record the excess displacement after puncturing through the peritoneum in each trial, denoted as the error. Additionally, we evaluated the total elapsed time of each trial, beginning when any force is applied and ending after puncturing the peritoneum and relieving all applied force. We expected the force vs. displacement plot to somewhat match previous studies on trocar insertion force profiles.²⁰ We also expected the error and elapsed time to decrease with subsequent trials. From these measurements, we can determine if the novice is learning from the trocar simulator.

5. RESULTS

Analyzing the mean force-displacement gathered across all trials in Fig. 5, a resemblance can be seen to the characteristic curve shown in Fig. 4. The force and displacement values at the puncture events on the experimental data curve closely match values gathered from a constant velocity trocar insertion on real tissue. However, because subjects were instructed to steadily increase their force as opposed to the constant velocity input used to obtained the characteristic curve, the reduction in force after a puncture event cannot be seen in the experimental data curve. Instead, the puncture events are found at points with a change in the slope of the curve, as a decrease in the slope of the curve corresponds to a drop in stiffness. The puncture events are denoted as the dashed lines, and the phases are labeled with the numerals in Fig. 5.

The linear actuators by themselves could not portray the sudden drop to the participants. Without the upper module, the users did not know when to stop applying force. Including the upper module in the trocar simulator rectified this issue .

As shown in Fig. 6, there is a slight decrease in error over the course of five trials. The data was tested for skewness and as a result, the data can be assumed to be from a normal distribution, enabling the use of a t-test statistic. When only observing the first and fifth trial, we perform a t-test for both of the conditions, and find a significant difference in the displacement error with visualization (p = 0.048), but not without visualization (p= 0.094). As these are independent conditions, an ANOVA test was used to determine significant differences. When performing an ANOVA test to include all of the trials, neither condition is found to contain a significant difference (p = 0.197, 0.705). We normalized each subject's error at each trial, dividing by the subject's mean error for that condition, with Fig. 7 showing the resulting bar graph. Each subject's mean error can be found in Table 1. The normalized error depicts a much more significant decrease across all trials. Performing an ANOVA test with the normalized data yields a significant difference for both conditions (p = 0.0005, 0.036). Finally, for the elapsed time per trial bar graph seen in Fig. 8, there is no significant difference in elapsed time for either with or without utilizing the visualization when performing an ANOVA test (p = 0.99, 0.97).

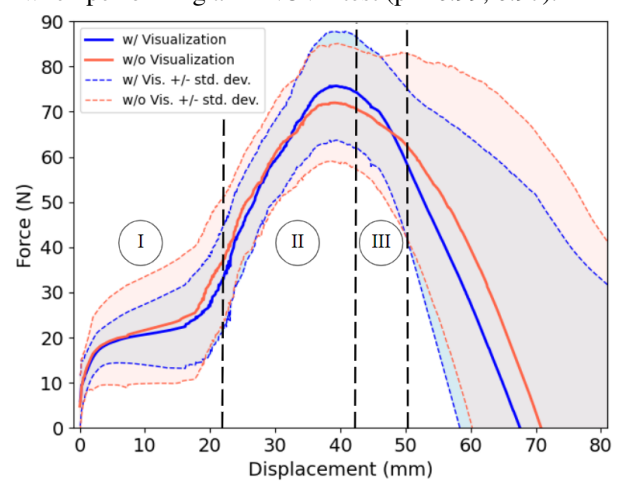


Fig. 5: Mean Force-Displacement curve of data gathered across all subjects and trials.

Paired t-tests between the two conditions were performed for the error, normalized error, and elapsed time data. None of the tests showed a significant difference between using and not using the visualization. Due to the large volume of entirely insignificant p-values from these tests, the p-values will not be listed. No significant results were due to subject gender.

Shown in Table 1, three out of the eight subjects had a higher mean error for the visualization condition, and of those three, only one had a difference between the two errors greater than 10%. Of the five subjects who had a lower mean error for the visualization condition, all of them had a difference between the two errors greater than 10%, with most falling in the 20% to 30% range.

In the post-experiment survey, all subjects rated the difficulty of using the trocar simulator as moderate or easier than moderate difficulty. All subjects also agreed or strongly agreed that holding the model trocar feels similar to holding a real trocar provided to them.

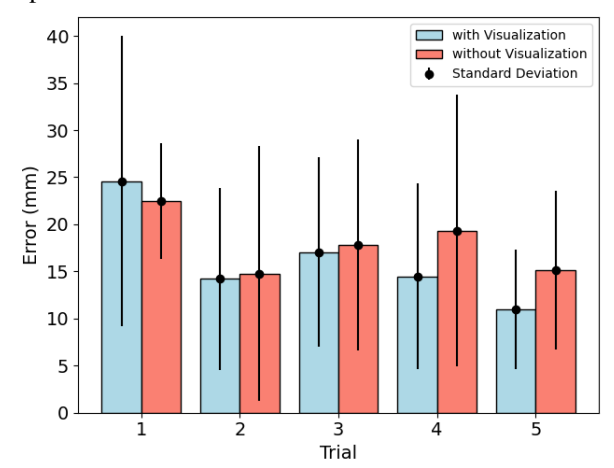


Fig. 6: Error (Excess Displacement) per Trial.

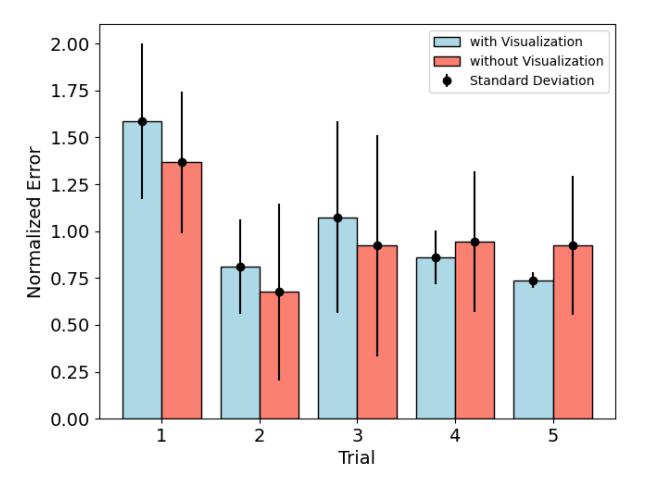


Fig. 7: Normalized Error per Trial. Error values are normalized by dividing by the subject's average error for that condition.

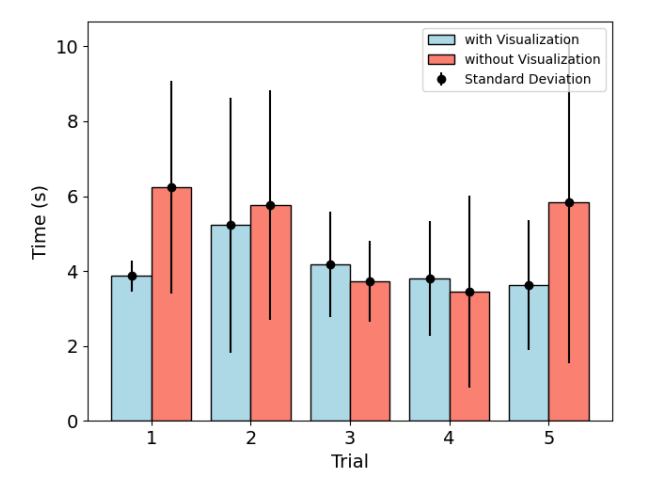


Fig. 8: Elapsed Time per Trial.

Table 1: Subject Mean Errors (mm) per Condition. '*' denotes which condition the subject performed first.

Subject	1	2	3	4
with Visualization	30.58	11.64*	25.20	7.67
without Visualization	28.38*	18.87	32.31*	9.54*

Subject	5	6	7	8
with Visualization	12.94*	5.14*	27.48	7.47*
without Visualization	17.08	7.37	18.27*	6.99

6. DISCUSSION

The mean force-displacement curve gathered from all trials, shown in Fig. 5, follows the same overall trend as the characteristic curve in Fig. 4, but there are some key differences. The ending to phase 1 is less clearly defined, as some subjects continued to increase their force after the first puncture event, so the sudden decrease in force is absent. Similarly, the final puncture event was passed suddenly by all subjects, due to their novice level at the task and the final puncture event's close proximity and lower necessary force in relation to the second puncture event. As such, the third puncture event is not clearly defined in the mean force-displacement curve. However, the peak force at the second puncture event is clearly visibly in mean curve near the absolute maximum, and a decline of force begins afterwards, slightly increasing in steepness after the final puncture event.

Compared to the prior iteration of the device, ¹² the new trocar simulator is able to better provide the forces necessary to simulate the end of the procedure. The previous iteration renders a maximum possible force of close to 70 N, posing a challenge to render some trocar insertion methods and models. ²⁰ Meanwhile, Fig. 5 depicts a maximum force of around 90 N in this study, and the device has the capability to render greater forces, showing this iteration is more versatile in simulating a variety of methods or scenarios. Furthermore, the larger workspace allows the simulation of a trocar insertion on obese patients, which was previously not possible.

Additionally, the upper module overcame an obstacle with admittance type haptic devices: the inability to render free space. Without rendering free space, the proper feedback could not be provided to the user, and the trocar simulator would not provide sufficient training in the procedure. The upper module provides the integral region of free space that is key in simulating the kinesthetic feedback found in a trocar insertion procedure.

We expected the visualization to assist in the learning process and result in lower error and elapsed time by the final trial. However, each subject's natural inclination to the task impacted their beginning and average error. As such, the raw error data does not depict the whole picture as to whether each subject is learning during their time utilizing the device. Accounting for differences between subject performance, the normalized error data in Fig. 7 more clearly depicts that each subject decreases

their error by the end of the five trials, particularly with subject error in the final visualization trial spread tightly around 75% of the subject's mean error after beginning with a mean close to 160% of the subject's mean error. Thus, with the visualization, subjects decreased their error by roughly 85% on average relative to themselves. A large portion of the error reduction occurs between the 1st and 2nd trials, but subjects showed an error decrease of close to 30% between the 2nd and final trials as well. The continued improvement is indicative of each subject learning as they used the trocar simulator. Furthermore, the novices were able to decrease their error without a significant increase in time, suggesting the subject is learning during the experiment and leading to an overall increase in performance. However, all subjects completed a trial much faster than the typical 20 to 30 seconds for a surgeon to complete the procedure. ²⁰ The fast times may be increasing the novices' error, but it does not detract from the subjects learning across the trials. Rather, slowing down may further increase a user's performance. During real surgery, subjects are likely to be much more careful than with this simulator, thus future work to add realism and a sense of criticality is important.

Although the paired t-tests did not indicate a significant difference in performance between two conditions, it is worth noting that the trials without the visualization performed better towards the earlier trials than the corresponding trials with the visualization, likely due to an acclamation period for the user. However, in the later trials, the condition with the visualization outperformed the condition without the visualization. Additionally, the subject mean errors with the visualization tended to be lower than subject mean errors without the visualization. As such, it is possible that prolonged testing may lead to an increase in the difference between the two conditions. Because the trocar simulator does not have the appearance of a procedure on human tissue, the user may find difficulty in connecting their training to the real procedure. The visualization of the close up of each layer is very similar to the endoscopic camera view, so trainees know what to expect during the procedure, and can likely form an easier mental connection between the two.

Finally, velocity values were also recorded during the experiment, but all trials depicted the linear actuators retracting at their maximum speed following the final puncture event. As expected, these results suggest the linear actuators are too slow to properly render the region of little resistance following the final puncture event. Thus, our findings reinforce the need for the free space region allowed by the upper module, and properly compensating for the drawbacks of the linear actuators.

7. CONCLUSION AND FUTURE WORK

This paper presents a significant improvement to our previously developed, Steward-platform based trocar insertion training simulator, through the addition of novel visualization, a dropping mechanism to render free space motion, and more robust actuators. From the human subject testing, we demonstrate that users improve their performance and learn through repeated use of the trocar simulator. For future work, a 6 DOF force-torque sensor will be used to take advantage of all six degrees of free-

dom offered by the Stewart platform mechanism. In addition, to further validate the device, a study involving experts will help improve force levels and visualization fidelity of the system, as well as ensure that a distinct difference can be seen between expert and novice data to prove simulator validity. In this study, experts should test current training standards, such as synthetic tissue, in addition to the trocar simulator, in order to compare their results and user experience with both training methods. Additional future work will include designing the upper module in a way that will allow it to be used in a continuous fashion to enable force drops between layers. To determine the long-term effects of training with the trocar simulator, a lengthier study with novices across several weeks, with a final trial excluding the visualization, should occur. Finally, either physically or in the visualization, the secondary effects of the simulator should be improved to assist users in connecting their training simulation performance to that of a real procedure. Integrating more realism may help subjects perform the task slower which will likely improve device performance as well.

8. ACKNOWLEDGEMENTS

We thank the NSF REU program for supporting this work, as well as Aldo Galvan, Allen Hewson, and Kyle Woo with the HeRo laboratory for helping to lay the groundwork for this project.

References

- [1] R. Agha and G. Muir, "Does laparoscopic surgery spell the end of the open surgeon?" *Journal of the Royal Society of Medicine*, vol. 96, no. 11, pp. 544-546, Nov. 2003.
- [2] S. Krishnakumar and P. Tambe, "Entry complications in laparoscopic surgery," *Journal of Gynecological Endoscopy and Surgery*, vol. 1, no. 1, pp. 4-11, 2009.
- [3] H. M. Elbiss and F. M. Abu-Zidan, "Bowel injury following gynecological laparoscopic surgery," *African Health Sciences*, vol. 17, no. 4, pp. 1237-1245, Dec. 2017.
- [4] J. Wind et al., "Medical liability insurance claims on entry-related complications in laparoscopy," *Surgical Endoscopy*, vol. 21, pp. 2094–2099, 2007.
- [5] R. Kassir et al., "Laparoscopic entry techniques in obese patients: Veress needle, direct trocar insertion or open entry technique?" *Obesity surgery*, vol. 24, pp. 2193–2194, 2014.
- [6] M. Coşkun and A. Yüksel, "Bladeless optical trocar insertion technique for initial access in morbidly obese patients: Technique and results," *Laparosc Endosc Surg Sci*, vol. 27, no. 4, pp. 193-198, 2020.
- [7] C. Rabl, F. Palazzo, H. Aoki, and G. M. Campos, "Initial Laparoscopic Access Using an Optical Trocar Without Pneumoperitoneum Is Safe and Effective in the Morbidly Obese," *Surgical Innovation*, vol. 15, no. 2, pp. 126-131, 2008
- [8] H. T. Sharp et al., "Complications associated with optical-access laparoscopic trocar," *Obstetrics & Gynecology*, vol. 99, no. 4, pp. 553–555, 2002.

- [9] R. Agha and A. J. Fowler, "The role and validity of surgical simulation," *International Surgery*, vol. 100, no. 2, pp. 350-357, 2015.
- [10] Y. W. Seo, A. Chowriappa, A. Abraham, K. Guru, and T. Kesavadas, "Methodology for haptic modeling of trocar insertion procedure," in ASME International Mechanical Engineering Congress and Exposition, vol. 56215, p. V03AT03A071, 2013.
- [11] Y. W. Seo, A. Chowriappa, K. Guru, and T. Kesavadas, "TroSim: New Haptic Simulator for Trocar Insertion Procedure," in SAGES 2013, 2013.
- [12] A. Galvan, A. K. Da Costa, J. Shields, K. Kho, and A. M. Fey, "Haptic simulator for trocar insertion training," in *IEEE World Haptics Conference*, 2021, pp. 397-402.
- [13] A. Q. Keemink, H. van der Kooij, and A. H. Stienen, "Admittance control for physical human–robot interaction," *The International Journal of Robotics Research*, vol. 37, no. 11, pp. 1421–1444, 2018.
- [14] K. Harib and K. Srinivasan, "Kinematic and dynamic analysis of Stewart platform-based machine tool structures," *Robotica*, vol. 21, pp. 541-554, 2003.
- [15] E. L. Faulring, J. E. Colgate, and M. A. Peshkin, "The Cobotic Hand Controller: Design, Control and Performance of a Novel Haptic Display," *The International Journal of Robotics Research*, vol. 25, no. 11, pp. 1099-1119, 2006.
- [16] M. Lin and M. Otaduy (Eds.), *Haptic Rendering*. New York: A K Peters/CRC Press, 2008.
- [17] R. J. Adams and B. Hannaford, "Stable haptic interaction with virtual environments," *IEEE Transactions on Robotics and Automation*, vol. 15, no. 3, pp. 465-474, June 1999.
- [18] T. Charters, R. Enguica, and P. Freitas, "Detecting Singularities of Stewart Platforms," *Mathematics-in-Industry Case Studies Journal*, vol. 1, pp. 66-80, 2009.
- [19] F. Conti, F. Barbagli, D. Morris, and C. Sewell, "Chai 3d: An open-source library for the rapid development of haptic scenes," in *IEEE World Haptics*, 2005, pp. 21-29.
- [20] J. Sun and K. Tadano, "Force characteristics and effective stopping upon the wall is penetrated out by trocar during laparoscopic surgery," *Journal of Mechanics in Medicine and Biology*, vol. 18, no. 03, 2018.
- [21] F. G. Hamza-Lup, C. M. Bogdan, D. M. Popovici, and O. D. Costea, "A Survey of Visuo-Haptic Simulation in Surgical Training," 2010.



Andres Hassun received his B.S. degree from The University of Texas at Austin in 2023. Now, he is pursuing his M.S. degree in Mechanical Engineering at The University of Texas at Austin under the supervision of Dr. Ann Majewicz Fey in the Human-Enabled Robotic Technology Lab.

This is the first publication for Andres Hassun. His research

interests include Haptics, surgical training systems, and surgical robotics.



Kimberly Kho received a B.A. in English and Asian Studies at Rice University, followed by M.D. at Baylor College of Medicine, M.P.H. from Harvard School of Public Health, M.Sc. from UT Southwestern. She completed residency in Obstetrics and Gynecology at Columbia University Medical Center and

fellowship in Minimally Invasive Gynecology Surgery at the Atlanta Center for Reproductive Medicine and Minimally Invasive Surgery.

She is a Professor of Obstetrics and Gynecology at the University of Texas Southwestern Medical Center and Director of the Fellowship in Minimally Invasive Gynecologic Surgery. Her research focuses on the evaluation of surgical interventions and introduction of new technologies in gynecologic care.



M. Yvette Williams-Brown received a B.S. in Biology at Xavier University, followed by an M.D. at Tulane University School of Medicine and a Master of Medical Science from the University of Texas Medical Branch at Galveston. She completed residency in Obstetrics and Gyne-

cology and a fellowship in Gynecologic Oncology also at the University of Texas Medical Branch at Galveston.

She is an Associate Professor in the Department of Women's Health at the Dell Medical School within the University of Texas at Austin and is the Program Director of the Minimally Invasive Gynecologic Surgery Fellowship program. Her research focuses on cervical cancer, palliative care, and health disparities.



Ann Majewicz Fey (Member, IEEE) received the B.S. degrees in Mechanical Engineering and Electrical Engineering from the University of St. Thomas, St. Paul, MN, in 2008, the M.S. degree in Mechanical Engineering from Johns Hopkins University, Baltimore, MD, in 2010, and the Ph.D. degree from Stanford University, Stanford, CA, in 2014, all in me-

chanical engineering.

She is currently an Assistant Professor of mechanical engineering at the University of Texas at Austin, Austin, TX, where she holds a joint appointment in the Department of Surgery at UT Southwestern Medical Center, Dallas, TX. She directs the Human-Enabled Robotic Technology (HeRo) Laboratory where she is responsible for research projects in the areas of robotassisted surgery, teleoperation, haptics, and human-centric modeling.

Dr. Majewicz Fey received the 2015 National Science Foundation CISE Research Initiation Initiative (CRII) award and the 2019 National Science Foundation CAREER Award.